

# MAGNETOSTRUCTURAL RELATIONSHIPS FOR Fe(III) SPIN CROSSOVER COMPLEXES

PETER AUGUSTÍN<sup>1</sup>, ROMAN BOČA<sup>2</sup>

<sup>1</sup>*Institute of Inorganic Chemistry, Faculty of Chemical and Food Technology, Slovak University of Technology, SK-812 37 Bratislava, Slovakia*

<sup>2</sup>*Department of Chemistry, University of SS. Cyril and Methodius in Trnava, SK-917 01 Trnava, Slovakia (roman.boca@stuba.sk)*

**Abstract:** Structural data for fifteen complexes of Fe(III) of a general formula  $[\text{FeL}^5\text{X}]$ , with pentadentate Schiff-base ligands  $\text{L}^5$  and unidentate coligands  $\text{X}^-$ , were subjected to a statistical analysis. The multivariate methods such as Pearson correlation, cluster analysis and principal component analysis split the data into two clusters depending upon the low-spin and/or high-spin state of the complex at the temperature of the X-ray experiment. Some of these complexes exhibit a thermally induced spin crossover. The numerical analysis of the magnetic susceptibility and magnetization data for an enlarged set of Fe(III) spin crossover systems yields the enthalpy  $\Delta H$  and entropy  $\Delta S$  of the transition along with the transition temperature  $T_{1/2}$  and the solid state cooperativeness. The thermodynamic data show a mutual relationship manifesting itself by linear  $\Delta S$  vs  $\Delta H$  and  $T_{1/2}$  vs  $\Delta H$  correlations.

**Key words:** spin crossover, Fe(III) complexes, structural and magnetic data, magnetostructural relationships

## 1. Introduction

A number of studies confirm a presence of thermally induced spin crossover between the low-spin (LS,  $S = 1/2$ ) and high-spin (HS,  $S = 5/2$ ) states in Fe(III) complexes (e.g. HALCROW *et al.*, 2013). This process can be viewed as a unimolecular, entropy driven reaction for which  $\Delta H > 0$  and  $\Delta S > 0$  is characteristic. The minimum value of  $\Delta S$  is represented by a pure electronic spin contribution  $\Delta S = R \ln(6/2) = 9.1 \text{ J K}^{-1} \text{ mol}^{-1}$  that is enriched by the vibrational contribution. The transition temperature, when the mole fraction obeys  $x_{\text{LS}} = x_{\text{HS}} = 0.5$ , is given by the ratio  $T_{1/2} = \Delta H/\Delta S$  and in order to get a sufficiently high value, say  $T_{1/2} > 100 \text{ K}$ , the lowest estimate for the enthalpy of the spin transition is  $\Delta H > 0.9 \text{ kJ mol}^{-1}$ .

These thermodynamic data can be measured by calorimetry (SORAI, 2002) but they are available also from an analysis of magnetic data such as temperature dependence of the magnetic susceptibility (BOČA *et al.*, 2003; PAVLIK *et al.*, 2013).

It was reported recently that the spin transition can be tuned by varying coligands in the basic skeleton of the complexes of  $[\text{Fe}^{\text{III}}\text{L}^5\text{X}]$  type; here  $\text{L}^5$  stands for a pentadentate Schiff base whereas  $\text{X}^-$  is a monodentate pseudohalido coligand (KRÜGER *et al.*, 2013; KRÜGER *et al.*, 2015; MASÁROVÁ *et al.*, 2015; NEMEC *et al.*, 2011; ŠALITROŠ *et al.*, 2009). Although chemists try to rationalize  $\Delta H$  by changing the ligand field strength, the aspects influencing the  $\Delta S$  cofactor are unclear so far. To our hypothesis some magnetostructural relationships could bring an answer of how to get the spin crossover with a desired transition temperature.

## 2. Material and methods

The pentadentate ligands  $H_2L^5$  were prepared by a Schiff condensation between the substituted salicylaldehyde (*Y-sal*) and the asymmetric triamine *pet* = 1,6-diamino-4-azaheptane as described elsewhere (KRÜGER *et al.*, 2013; NEMEC *et al.*, 2011). Their Fe(III) complexes  $[Fe(Y-salpet)X]$  were prepared by published recipes (see Fig. 1) where the Fe(III) salt was combined with  $H_2L^5$  and pseudohalide  $X^-$  ligands. The elemental analysis confirmed the composition of the complexes.

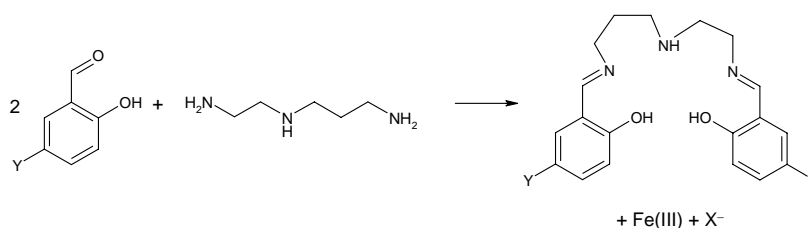


Fig. 1. Synthetic route for preparing Fe(III) complexes of the  $[FeL^5X]$  type; Y = Cl and Br,  $X^- = Cl^-, N_3^-, NCO^-, NCS^-$  and  $NCS_2^-$ .

Single crystals were subjected to the X-ray structure analysis and the results can be retrieved from the Cambridge Structural Database. The measured interatomic distances within the  $\{FeN_2N'O_2X\}$  chromophore are listed in Table 1.

Table 1. Structural parameters for Fe<sup>III</sup> complexes under study.<sup>a</sup>

Compound	Class	Fe-N <sub>am</sub>	Fe-N <sub>im</sub>	Fe-O	Fe-X	Σ	α
1 [Fe(L <sup>Br</sup> )(Cl)]·0.5H <sub>2</sub> O	H	2.188	2.088	1.959	2.352	62.3	63.1
2 [Fe(L <sup>Br</sup> )(NCS)]	H	2.207	2.099	1.927	2.111	56.3	67.7
3 [Fe(L <sup>Br</sup> )(N <sub>3</sub> )]·MeOH	H, SC	2.183	2.113	1.942	2.048	72.3	35.0
4 [Fe(L <sup>Br</sup> )(NCS <sub>2</sub> )]	L, SC	2.013	1.952	1.884	1.944	27.8	85.9
5 [Fe(L <sup>Cl</sup> )(Cl)]·0.25H <sub>2</sub> O	H	2.199	2.095	1.958	2.361	66.9	62.2
6 [Fe(L <sup>Cl</sup> )(NCO)]	H	2.205	2.093	1.954	1.996	55.4	69.0
7 [Fe(L <sup>Cl</sup> )(NCS)]	L, SC	2.000	1.932	1.879	1.944	27.1	84.5
8 [Fe(L <sup>Cl</sup> )(NCS <sub>2</sub> )]	L, SC	2.001	1.932	1.881	1.952	26.9	85.5
9 [Fe(L <sup>Cl</sup> )(CN)]·H <sub>2</sub> O	L	2.012	1.934	1.903	1.959	19.3	65.9
10 [Fe(L)(CN)]·CH <sub>3</sub> OH	L	2.000	1.922	1.880	1.962	24.6	76.0
11 [Fe(3-Bu <sup>1</sup> ,5-Me-L)(NCS)]	H	2.191	2.096	1.916	2.100	56.0	75.6
12 [Fe(L <sup>m</sup> )(NCO)]·MeOH	H	2.218	2.078	1.946	2.081	54.0	73.3
13 [Fe(L <sup>m</sup> )(N <sub>3</sub> )]	H	2.211	2.085	1.936	2.085	57.4	58.1
14 [Fe(L <sup>m</sup> )(CN)]·MeOH	L	2.028	1.935	1.904	1.971	26.0	69.1
15 [Fe(L <sup>o</sup> )(CN)]·H <sub>2</sub> O	L	2.010	1.944	1.904	1.975	20.8	66.4

<sup>a</sup> Distances in Å, angles Σ and α in deg. Class – classification according to the temperature of the X-ray experiment in comparison with spin state: H – high-spin, L – low spin, SC – spin crossover. Octahedral distortion angle Σ is calculated from twelve *cis* angles within the chromophore. Angle α – between planes of aromatic rings. Abbreviations: L = *salpet*, L<sup>Cl</sup> = 5-Cl-*salpet*, L<sup>Br</sup> = 5-Br-*salpet*, L<sup>m</sup> = 3-MeO-*salpet*, L<sup>o</sup> = 3-EtO-*salpet*. References: KRÜGER *et al.*, 2013; KRÜGER *et al.*, 2015; MASÁROVÁ *et al.*, 2015; NEMEC *et al.*, 2011; ŠALITROŠ *et al.*, 2009.

The SQUID magnetometer (Quantum Design, MPMS-XL7) was used for measurements of the magnetic data (temperature dependence of the magnetic

susceptibility, and field dependence of the magnetization). The magnetic data for Fe<sup>III</sup> complexes referring either to the low-spin (LS) or the high-spin (HS) state was analyzed in terms of the Curie-Weiss law; to this end the g-factor, Weiss constant  $\Theta$ , and the van Vleck term  $\alpha$  were obtained. Some systems exhibit a thermally induced spin crossover and those data was analyzed by using Ising-like model with vibrations (equivalent to the thermodynamic regular solution model) giving rise the enthalpy  $\Delta H$  and entropy  $\Delta S$  of the spin transition along with the transition temperature  $T_{1/2}$  and the solid-state cooperativeness  $\Gamma$  (BOČA *et al.*, 2003; PAVLIK *et al.*, 2013). These data is listed in Table 2 along with some literature sources.

Table 2. Thermodynamic parameters for spin crossover complexes under study.<sup>a</sup>

	<b>Compound</b>	<b>Type</b>	<b><math>T_{1/2}/\text{K}</math></b>	<b><math>\Delta H/\text{kJ mol}^{-1}</math></b>	<b><math>\Delta S/\text{J K}^{-1} \text{mol}^{-1}</math></b>	<b><math>(\Gamma/k_B)/\text{K}</math></b>
<b>1</b>	[Fe(L <sup>Ct</sup> )(NCS)]	SC	280	5.77	20.6	180
<b>2</b>	[Fe(L <sup>Ct</sup> )(NCSe)]	SC	293	6.54	22.3	197
<b>3</b>	[Fe(L <sup>Br</sup> )(N <sub>3</sub> )]·CH <sub>3</sub> OH	SC	142	1.64	11.5	76
<b>4</b>	[Fe(L <sup>Br</sup> )(NCSe)]	SC	326	6.03	18.5	215
<b>5</b>	[Fe(L <sup>S</sup> )(NCS)]	SC	84, 82	2.07	(5.0)	90
<b>6</b>	[Fe(5Cl- <i>saldpm</i> )py]BPh <sub>4</sub>	SC*	78	0.44	5.61	63
<b>7</b>	[Fe(3m- <i>saldpm</i> )py]BPh <sub>4</sub>	SC	273	4.54	16.6	90
<b>8</b>	[Fe( <i>saldpm</i> )py]BPh <sub>4</sub>	SC	310	5.42	17.5	150
<b>9</b>	[Fe( <i>napet</i> )(N <sub>3</sub> )]·MeOH	SC	122, 117	1.53	11.2	99
<b>10</b>	[Fe( <i>napet</i> )(NCS)]·MeCN	SC	151	1.92	12.5	87
<b>11</b>	[Fe( <i>napet</i> )(NCS)]	SC	180	0.90	(5.0)	135
<b>12</b>	[Fe( <i>napet</i> )(NCO)]	SC	155	2.54	16.3	102
<b>13</b>	[Fe( <i>napet</i> )(NCSe)]·MeCN	SC	170	2.29	13.3	99

<sup>a</sup> SC – spin crossover between spins 1/2  $\rightarrow$  5/2, SC – with hysteresis. SC\* - spin crossover between spins 3/2  $\rightarrow$  5/2. Abbr. for ligands: *saldpm* = *N,N'*-bis(2-hydroxybenzyliden)-1,7-diamino-4-azaheptane, *napet* = *N,N'*-bis(2-hydroxynaphthylidene)-1,6-diamino-4-azahexane. References: BOČA *et al.*, 2000; KRÜGER *et al.*, 2013; KRÜGER *et al.*, 2015; MASÁROVÁ *et al.*, 2015; NEMEC *et al.*, 2011; ŠALITROŠ *et al.*, 2009.

### 3. Results and discussion

The structural data was analyzed by using the statistical tools of the multivariate methods (STATGRAPHICS Centurion XV, 2006): the Cluster Analysis (CA), the Principal Component Analysis (PCA), and the Pearson Correlation (PC).

The cluster analysis (using Ward's method, distance according to the square Euclidean norm) shows that the data is split into two principal clusters according to their similarity (Fig. 2). Centroids of the two clusters are listed in Table 3. It can be seen that all distances in the cluster 1 are higher than in cluster 2 which allows concluding that the cluster 1 involves high-spin complexes (complexes which are high-spin at the temperature of the X-ray experiment). Then the cluster 2 contains low-spin complexes.

Table 3. Centroids of the parameters according to the cluster analysis.

<b>Cluster</b>	<b>Fe-N<sub>am</sub></b>	<b>Fe-N<sub>im</sub></b>	<b>Fe-O</b>	<b>Fe-X</b>	<b><math>\Sigma</math></b>	<b><math>\alpha</math></b>
1	2.200	2.093	1.942	2.142	60.07	63.0
2	2.009	1.936	1.891	1.958	24.64	76.2

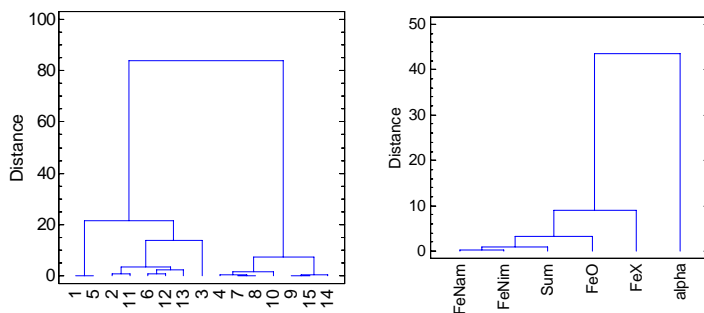


Fig. 2. Dendrograms of the cluster analysis. Left – for complexes; right – for distances and angles. Data according to Table 1.

The PCA method performs a linear transformation of the original parameters into principal components that bear the maximum information about the variability of data. Here the first component involves 79 % and the second one 11 % of the variability, in total 90 %. The diagram (Fig. 3) shows which variables correlate, anticorrelate, or do not correlate. It follows that the interatomic distances Fe-N<sub>am</sub>, Fe-N<sub>im</sub>, Fe-O mutually correlate and also they correlate with the parameter  $\Sigma$ . On the contrary,  $\alpha$ -parameter does not correlate with the others.

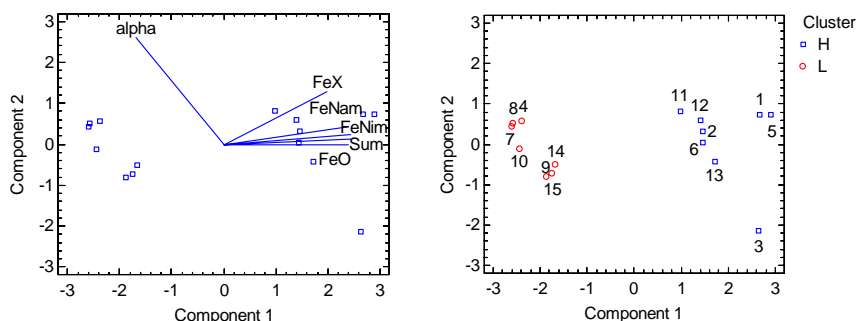


Fig. 3. Results of PCA. Left – a biplot with ray diagram, right – individual complexes classified into two clusters.

PCA also brings information about the distribution of the original objects and the corresponding graph is also display in Fig. 3. It unambiguously identifies that the cluster 1 (squares) contains high-spin complexes whereas the cluster 2 (circles) the low-spin ones (at the temperature of the X-ray experiment).

Finally, the PC analysis offers the pair correlation coefficients as listed in Table 4. Now it is seen that the greater Fe-N<sub>am</sub>, the greater Fe-N<sub>im</sub> and Fe-O. Also the octahedral distortion parameter  $\Sigma$  increases with distance of the amino nitrogen Fe-N<sub>am</sub> and also imino nitrogen Fe-N<sub>im</sub>. The angle of the aromatic rings  $\alpha$  does not display any significant correlation with the other structural parameters.

Table 4. Pair correlation (Pearson) coefficients for structural parameters.

	Fe-N <sub>am</sub>	Fe-X	Fe-N <sub>im</sub>	Fe-O	$\Sigma$	$\alpha$
Fe-N <sub>am</sub>		0.677	0.984	0.900	0.942	-0.515
Fe-X	0.677		0.683	0.757	0.732	-0.372
Fe-N <sub>im</sub>	0.984	0.683		0.885	0.972	-0.569
Fe-O	0.900	0.757	0.885		0.869	-0.639
$\Sigma$	0.942	0.732	0.972	0.869		-0.613
$\alpha$	-0.515	-0.372	-0.569	-0.639	-0.613	

The recorded temperature dependence of the effective magnetic moment for a number of complexes is displayed in Fig. 4 for a fixed pentadentate ligand L<sup>5</sup> and varied coligand X<sup>-</sup>. It can be seen that with increasing crystal field strength of the coligand X<sup>-</sup> (according to the well-known spectrochemical series) the spin states of complexes move from the high-spin behavior through the spin crossover behavior to the low-spin state.

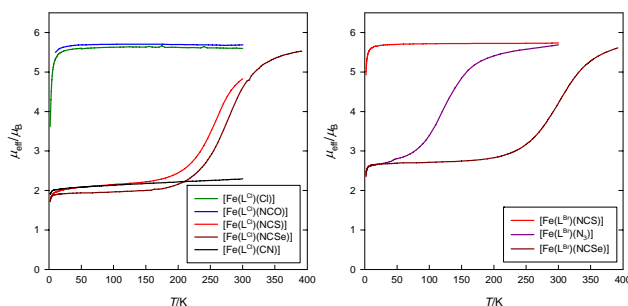


Fig. 4. Comparison of the spin crossover in  $[\text{Fe}^{\text{III}}\text{L}^5\text{X}]$  type complexes for a fixed Schiff-base ligand and varied coligand. For references see Table 2.

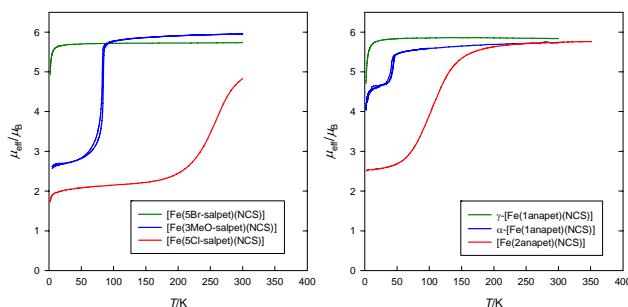


Fig. 5. Comparison of the spin crossover in  $[\text{Fe}^{\text{III}}\text{L}^5\text{X}]$  type complexes for a varied Schiff-base ligand and fixed coligand. For references see Table 2.

The spin state of the complex can be influenced also by the Schiff-base ligand with a fixed coligand as shown in Fig. 5 for  $\text{X}^- = \text{NCS}^-$ .

In order to find relationships among the thermodynamic parameters governing the spin crossover the multivariate statistical methods were applied: CA, PCA and PC. For

this purpose the data listed in Table 2 were employed. The results of the cluster analysis are presented in Fig. 6. It can be seen that they span two clusters with centroids characterized in Table 5. The cluster 1 involves complexes (No 1, 2, 4, 7, and 8) for which near- and above-room temperature spin crossover has been observed.

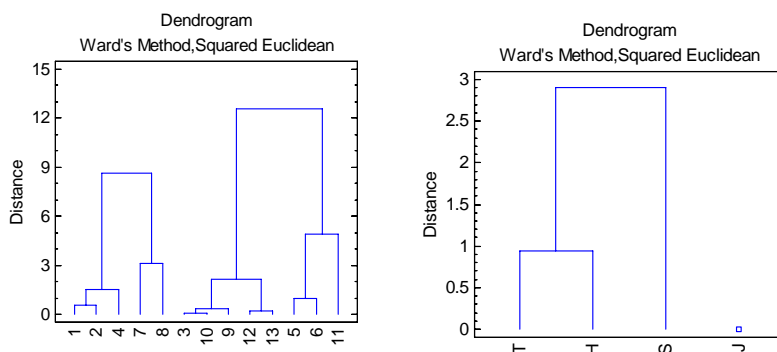


Fig. 6. Dendrograms of the cluster analysis. Left – for complexes, right – for thermodynamic parameters. Data according to Table 2.

Table 5. Centroids of the parameters according to the cluster analysis.

Cluster	$T = T_{1/2}$	$H = \Delta H$	$S = \Delta S$	$J = \Gamma$
1	296.4	5.66	19.1	166.4
2	134.9	1.67	10.1	93.9

The PCA analysis yields the diagrams presented in Fig. 7. It can be seen that the transition temperature  $T_{1/2}$  (abbr. T) correlates with the enthalpy of the transition  $\Delta H$  (abbr. H) whereas the correlation with the remaining parameters  $\Delta S$  (abbr. S) and  $\Gamma$  (abbr. J) is much weaker. The diagram on the right shows the objects classified into individual clusters.

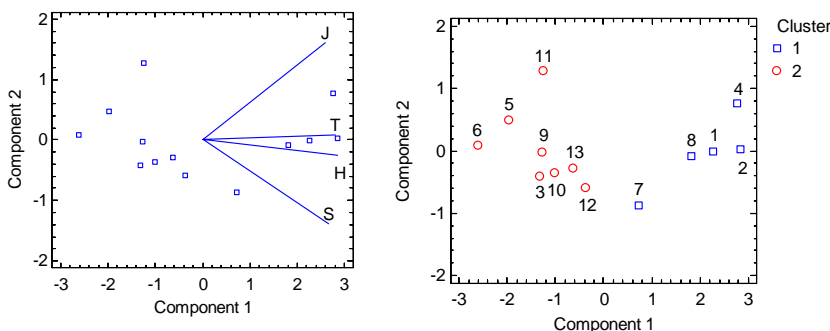


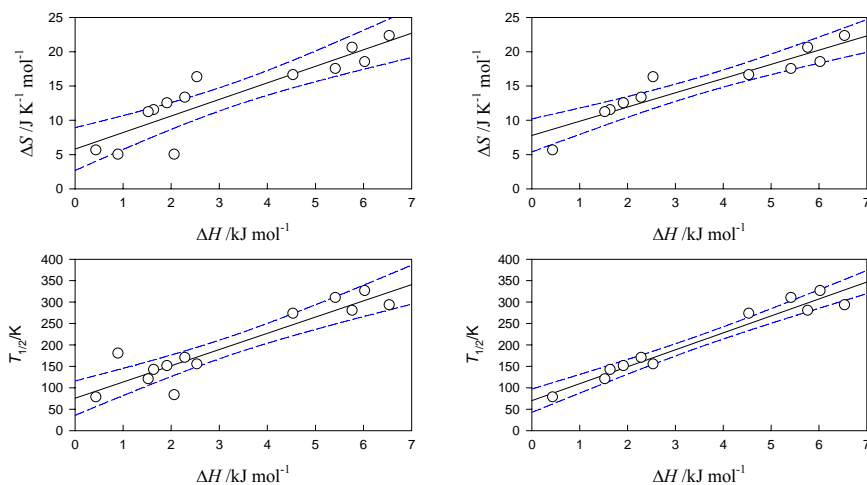
Fig. 7. Results of PCA. Left – a biplot with ray diagram, right – individual objects classified to the clusters (numbering according to Table 2).

The Pearson correlation yields the pair correlation coefficients listed in Table 6. It is confirmed numerically that the highest correlation coefficient refers to the  $T_c - \Delta H$  pair.

Table 6. Pair correlation (Pearson) coefficients for thermodynamic parameters.

	$T = T_{1/2}$	$H = \Delta H$	$S = \Delta S$	$J = \Gamma$
T		0.922	0.826	0.824
H	0.922		0.890	0.826
S	0.826	0.890		0.675
J	0.824	0.826	0.675	

The values of  $\Delta S$  were plotted versus the  $\Delta H$  and the corresponding graph is presented in Fig. 8 along with the linear regression curve and confidence intervals (95 %). Analogously, the values of  $T_{1/2}$  correlate with  $\Delta H$ . These correlations were replotted on the right side of Fig. 8 when points with a problematic value of  $\Delta S < 9.1 \text{ J K}^{-1} \text{ mol}^{-1}$  (complexes 5 and 11) were excluded from the correlation. The correlation is much improved.

Fig. 8. Linear correlations  $T_{1/2}$  vs  $\Delta H$  and  $\Delta S$  vs  $\Delta H$ . Right – reduced data omitting two problematic points.

## 4. Conclusions

It has been demonstrated that the structural parameters within the  $\{\text{FeN}_2\text{N}'\text{O}_2\text{X}\}$  chromophore of the  $[\text{Fe}^{\text{III}}\text{L}_5\text{X}]$  type complexes mutually correlate at a significant level. The complexes are classified into two clusters depending upon the low-spin and/or high-spin state of the complex at the temperature of the X-ray experiment. The thermodynamic data that characterize the spin crossover in the given class of Fe(III) complexes again show a mutual correlation confirmed by the multivariate methods. Again two principal clusters are visible, one for the systems exhibiting the spin crossover near- and above-room temperature, and the second for those showing the spin crossover below the room temperature. The enthalpy of the spin transition can be tuned by the coligand  $\text{X}^-$  and consequently also the transition temperature is a function of  $\Delta H$ . To this end, the coligands spanning the right side of the spectroscopic series

cause an increase in the enthalpy of the spin transition, and consequently a rising of the transition temperature towards and above the room temperature.

**Acknowledgements:** Slovak grant agencies (VEGA 1/0233/12, VEGA 1/0522/14 and APVV-14-0078) are acknowledged for the financial support.

## References

- BOČA, R., LINERT, W.: Is there a need for new models of the spin crossover? *Monats. Chemie*, 134, 2003, 199-216.
- BOČA, R., FUKUDA, Y., GEMBICKÝ, M., HERCHEL, R., JAROŠČIAK, R., LINERT, W., RENZ, F., Yuzurihara J.: Spin crossover in mononuclear and binuclear iron(III) complexes with pentadentate Schiff-base ligands. *Chem. Phys. Lett.*, 325, 2000, 411-419.
- CAMBRIDGE STRUCTURAL DATABASE, Cambridge Crystallographic Data Centre, Cambridge, CB2 1EZ, United Kingdom.
- HALCROW, M. A. (Ed.): *Spin-Crossover Materials: Properties and Applications*. Wiley, New York, 2013.
- KRÜGER, C., AUGUSTÍN, P., NEMEC, I., TRÁVNÍČEK, Z., OSHIO, H., BOČA, R., RENZ, F.: Spin crossover in iron(III) complexes with pentadentate Schiff-base ligands and pseudohalido coligands. *Eur. J. Inorg. Chem.*, 2013, 902-915.
- KRÜGER, C., AUGUSTÍN, P., DLHÁŇ, Ľ., PAVLIK, J., MONCOL, J., NEMEC, I., BOČA, R., RENZ, F.: Iron(III) complexes with pentadentate Schiff-base ligands: Influence of crystal packing change and pseudohalido coligand variations on spin crossover. *Polyhedron*, 87, 2015, 194-201.
- MASÁROVÁ, P., ZOUFALÝ, J., MONCOL, J., NEMEC, I., PAVLIK, J., GEMBICKÝ, M., TRÁVNÍČEK, Z., BOČA, R., ŠALITROŠ, I.: Spin crossover and high spin electroneutral mononuclear iron(III) Schiff base complexes involving terminal pseudohalido ligands. *New. J. Chem.*, 39, 2015, 508-519.
- NEMEC, I., HERCHEL, R., BOČA, R., TRÁVNÍČEK, Z., SVOBODA, I., FUESS, H., LINERT, W.: Tuning of spin crossover behaviour in iron(III) complexes involving pentadentate Schiff bases and pseudohalides. *Dalton Trans.*, 40, 2011, 10090-10099.
- PAVLIK, J., BOČA, R.: Established static models of the spin crossover. *Eur. J. Inorg. Chem.*, 2013, 697-709.
- SORAI, M.: Calorimetric investigations of phase transitions in which electrons are directly involved. *J. Chem. Thermodyn.*, 34, 2002, 1207-1253.
- STATGRAPHICS CENTURION XV. Statpoint Inc., 2006.
- ŠALITROŠ, I., BOČA, R., DLHÁŇ, Ľ., GEMBICKÝ, M., KOŽÍŠEK, J., LINARES, J., MONCOL, J., NEMEC, I., PERAŠÍNOVÁ, L., RENZ, F., SVOBODA, I., FUESS, H.: Unconventional spin crossover in dinuclear and trinuclear iron(III) complexes with cyanido and metallacyanido bridges. *Eur. J. Inorg. Chem.*, 2009, 3141-3154.